THE STUDY OF THE KINEMATICS OF THE LIFTING-LOWERING MECHANISM OF THE SMA-2 POWERED ROOF SUPPORT USING COMPUTER SOFTWARE

ANDREI ANDRAŞ[1], FLORIN DUMITRU POPESCU[2], IONELA CRISTINA MĂCEŞARU (LĂPĂDUŞI)[3], ILDIKO BRÎNAŞ[4]

Abstract: The shield of the SMA-2 utilizes a quadrilateral mechanism with a corner cylinder generating a lemniscate. The synthesis of the quadrilateral mechanism, its geometric and kinematic analysis in correlation with the geometry and kinematics of the entire support, raises challenging analytical issues. For this reason, in the present work, we have theoretically and practically analyzed the geometry and kinematics of the mechanism, demonstrating the utility of using computer software for modeling and simulation in addressing these problems.

Keywords: Mechanized support, Bernoulli, speed, trajectory, mean square value.

1. BERNOULLI'S LEMNISCATE – THEORETICAL CONCEPTS

If two points called foci F_1 and F_2 are considered in the plane and R is half the distance between them, then Bernoulli's Lemniscate (Figure 1) is defined as the geometric location of points in the plane that have the property that the product of their distance from the two foci is equal to R^2:

$$\left[\left(x-R\right)^2+y^2\right]\cdot\left[\left(x+R\right)^2+y^2\right]=R^4 \Leftrightarrow \left(x^2+y^2\right)^2=2R^2\cdot\left(x^2-y^2\right) \tag{1}$$

If in equation (1) substitutions are introduced:

$$R=\frac{a}{\sqrt{2}};\quad y=x\cdot\sin\left(t\right) \tag{2}$$

[1] *Prof. Ph.D. Eng., University of Petroşani, fpopescu@gmail.com*
[2] *Prof. Ph.D. Eng., University of Petroşani, andrei.andras@gmail.com*
[3] *Ph.D. student Eng., University of Petroşani, cristinamacesaru@yahoo.com*
[4] *Lecturer Ph.D. Eng., University of Petroşani, kerteszildiko@ymail.com*

the parametric equations of Bernoulli's Lemniscate in relation to cartesian coordinate axes are obtained:

$$x = \frac{a \cdot \cos(t)}{1 + \sin^2(t)}$$
$$y = \frac{a \cdot \sin(t) \cdot \cos(t)}{1 + \sin^2(t)} \tag{3}$$

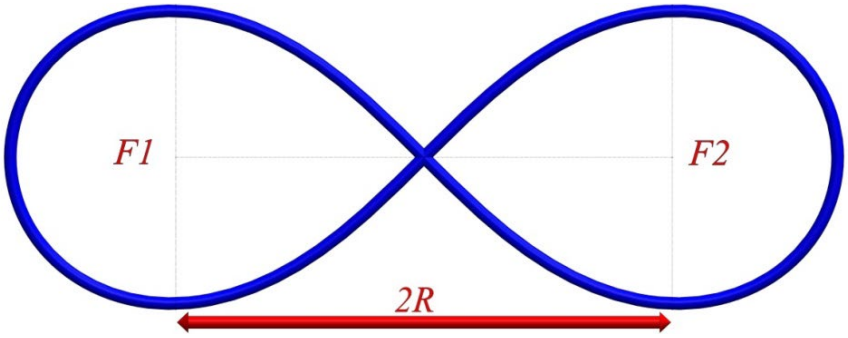

Fig. 1. Bernoulli's Lemniscate

The curve in Figure 1 was obtained using the SOLIDWORKS application by using `Sketch` module where a spline curve was drawn, implementing the parametric equations of lemniscate (Figure 2). The variable t in the parametric equations described in Figure 2 represents the angle that the position vector of points on the curve makes with the x-axis. The angle of the lemniscate curve in Figure 2 varies between 0 and π/4.

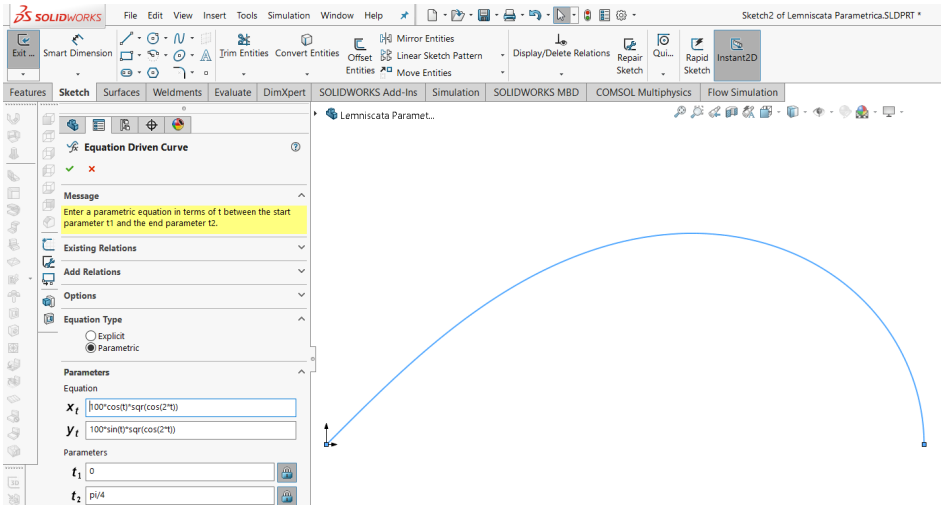

Fig. 2. Plotting the Bernoulli's Lemniscate in SOLIDWORKS

2. STUDY OF KINEMATICS OF A PLANAR QUADRILATERAL MECHANISM

The planar quadrilateral mechanism visible in Figure 3 was built using the SOLIDWORKS application. It consists of the fixed element 1, the driving element in the form of a crank 2, the driven element in the form of a connecting rod 3, and the rocker element 4. The mechanism in Figure 3 is an assembly consisting of parts 1, 2, 3, and 4. Property '`fix`' has been assigned to Element 1, and simple geometric constraints of concentricity have been established between adjacent elements. The motion of the mechanism is achieved by attaching a rotational motor (actuator) to driving element 2.

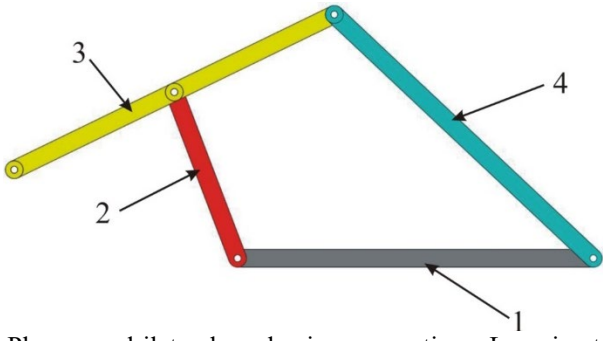

Fig. 3. Planar quadrilateral mechanism generating a Lemniscate curve

Its characteristics are presented in Figure 4, where the attachment mode of the driving element to crank 2 can be observed. The simulation time is 20 seconds, and the motor speed is 3 revolutions per minute. The kinematics study was conducted using `Motion Study` with the `Motion Analysis` submenu.

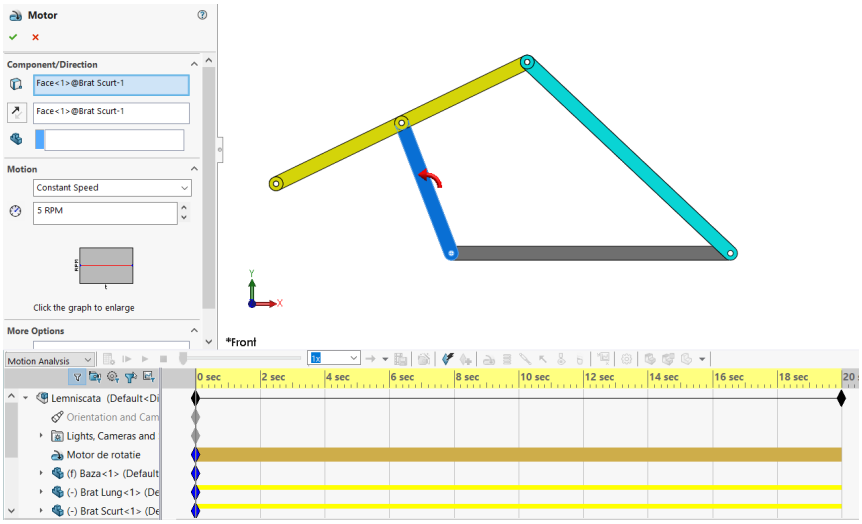

Fig. 4. Characteristics of the driving element drive motor

After performing the calculations, we plotted the trajectory of a point at the free end of the connecting rod (Figure 5).

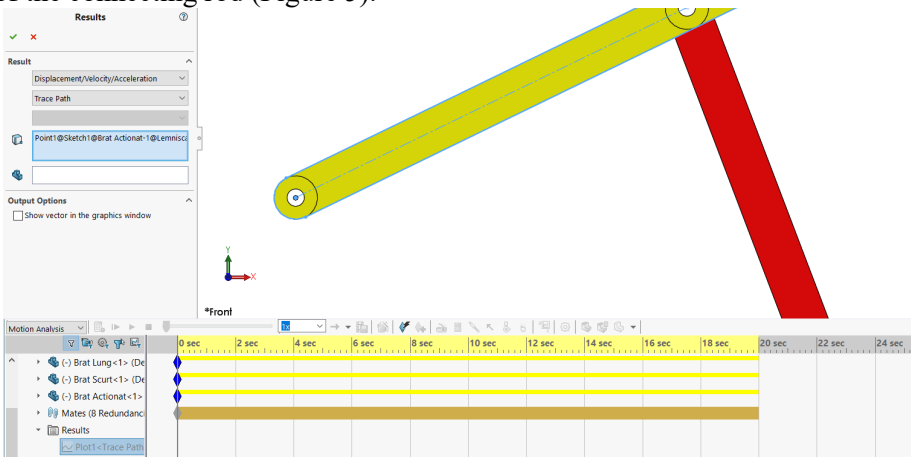

Fig. 5. Determination of the point for which the trajectory is plotted

The obtained trajectory is presented in Figure 6. It can be concluded that when the driving element 2 undergoes a rotational motion, the point at the free end of the driven connecting rod describes a Lemniscate-type trajectory.

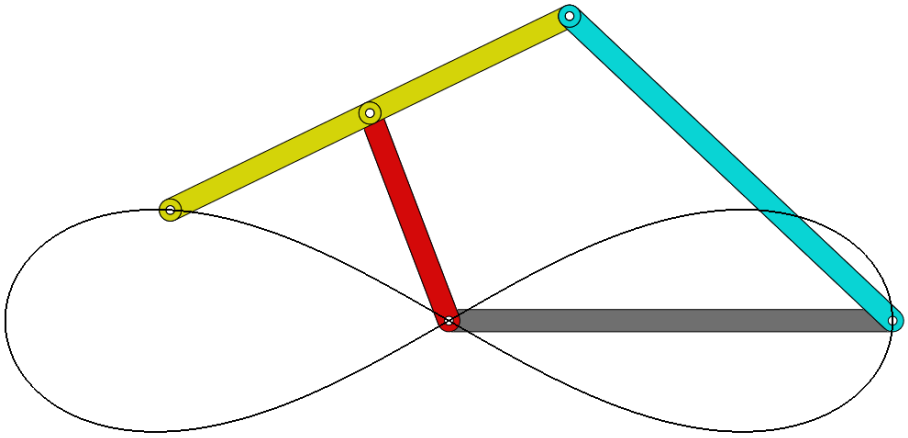

Fig. 6. Trajectory of the point at the free end of the driven element 3

In Figures 7a, 7b, 7c, and 7d, trajectories described by various points on the driven connecting rod are presented. In Figure 7a, the trajectory is described by the point located halfway between the free end of the connecting rod and its articulation point with the crank. It has the shape of an asymmetric Lemniscate. The trajectory of the point at the articulation of the connecting rod with the crank is shown in Figure 7b. As expected, the trajectory is a circle since the point describing it, is identical to the upper end of the crank. Figure 7c presents the trajectory of the point located in the middle of the distance

between the articulation points of the connecting rod with the crank and the rocker element. This is a closed curve. For the articulation point of the connecting rod with the rocker element, the trajectory is an arc of a circle, as the point undergoes a pendulum-like motion along this path.

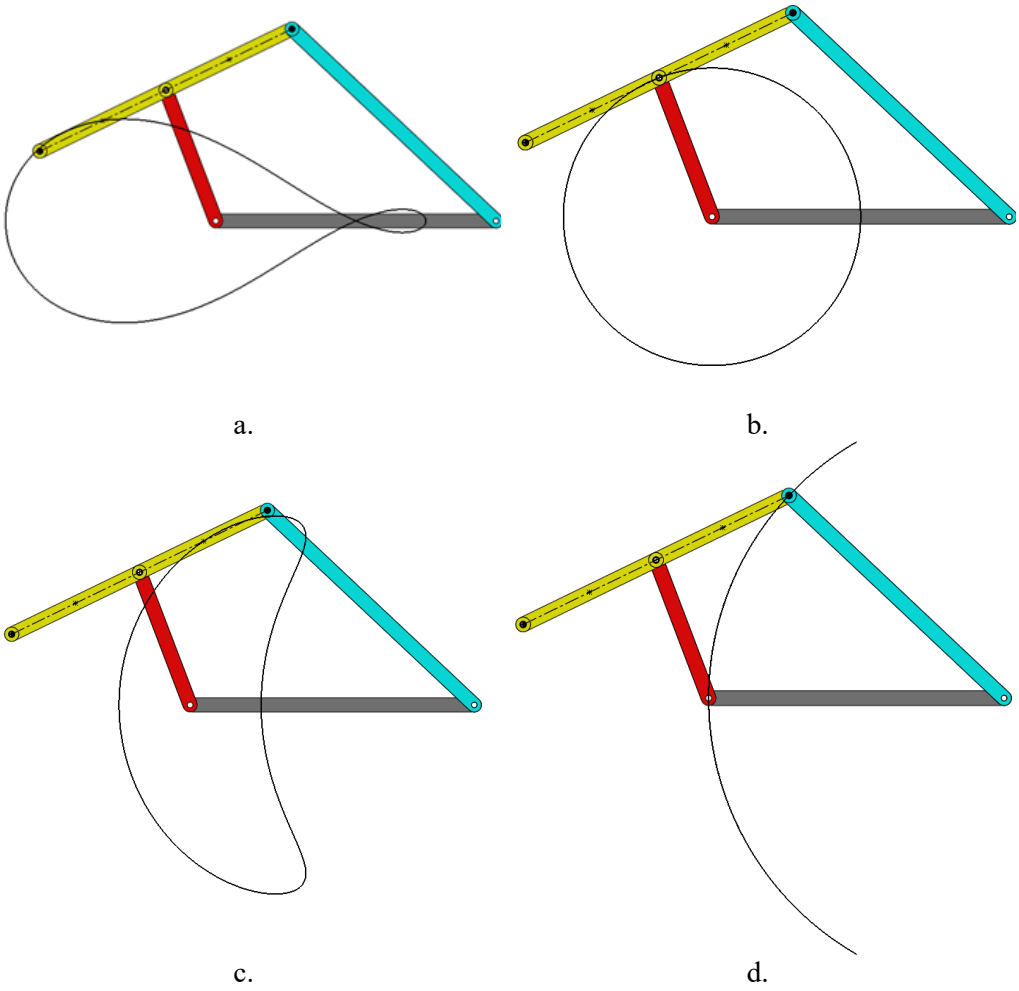

Fig. 7. The trajectories described by various points on the driven element 3

3. KINEMATICS STUDY OF THE MECHANIZED SUPPORT MODEL SMA-2

For the kinematics study of a mechanized support of type SMA-2, we utilized the model presented in Figure 8.

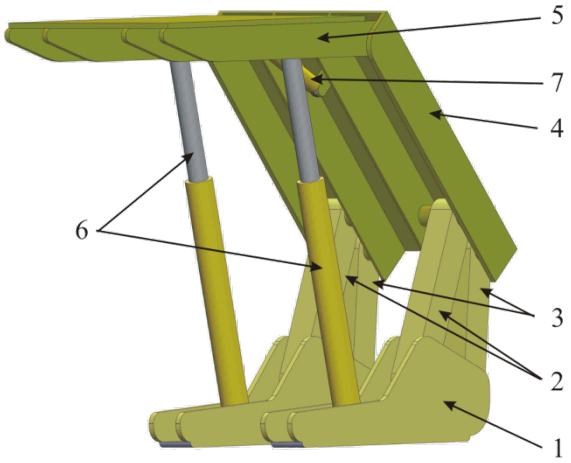

Fig. 8. The model of the mechanized support SMA-2 consists of: 1 – base, 2 – the long arm of the quadrilateral mechanism, 3 – the short arm of the quadrilateral mechanism, 4 – the shield, 5 – the beam, 6 - the hydraulic pillar, 7 – the corner hydraulic cylinder

The quadrilateral mechanism composed of the fixed base, the two arms, and the shield of the mechanized support is a double rocker mechanism since it satisfies Grashof's condition (Figure 9) for planar quadrilateral mechanisms (the sum of the maximum and minimum lengths of the elements must be less than or equal to the sum of the lengths of the other two elements).

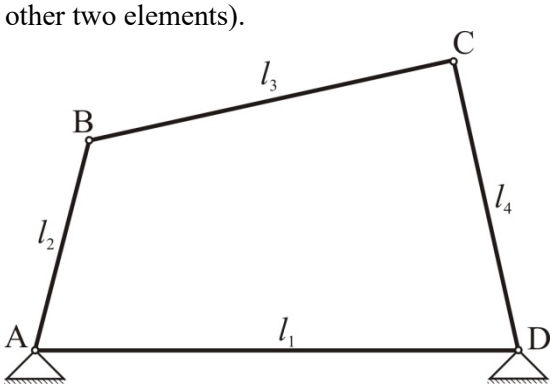

Fig. 9. Representation of the Grashof condition

If in the Figure 9, element $\overline{AB}$ has the minimum length of l_2, and element $\overline{AD}$ with the maximum length of l_1, then the Grashof condition is given by equation:

$$l_1 + l_2 \leq l_3 + l_4 \tag{4}$$

In the adopted model of the support, the base plays the role of the fixed element, the two supporting arms of the shield act as rockers, and the shield itself serves as the connection rod.

The base of the mechanized support was assigned the fixed property. The lifting-lowering motion of the support beam is achieved by attaching two linear motors (actuators) to one of the two hydraulic pillars. These act upon the pillar in accordance with the Gantt diagrams depicting the sequence of actuator actions in Figures 10 and 11.

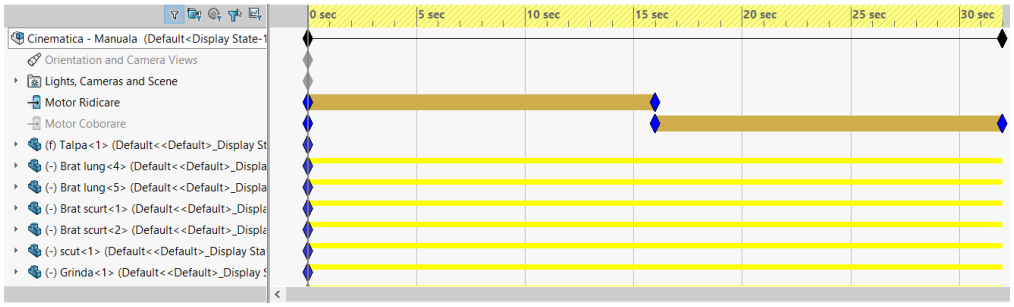

Fig. 10. Gantt diagram illustrating the sequence of actions for linear actuators (lifting motor is active, lowering motor is passive)

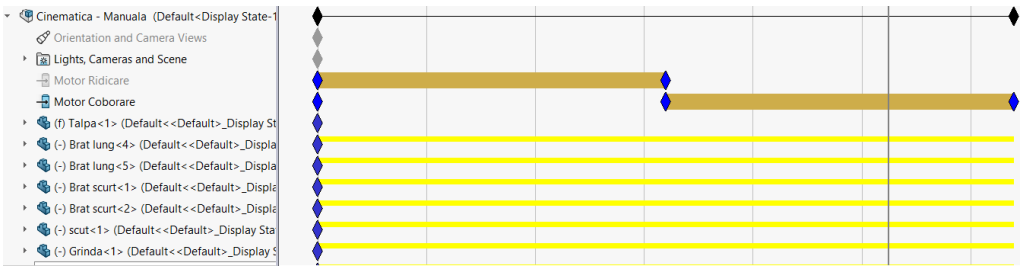

Fig. 11. Gantt diagram illustrating the sequence of actions for linear actuators (lifting motor is passive, lowering motor is active).

The time interval for kinematic study is 32 seconds. The lifting motor is active for the first 16 seconds of the simulation, during which the lowering motor is passive. After this time interval, the lowering motor becomes active, and the lifting motor becomes passive.

If both motors were active throughout the entire simulation period, the SOLIDWORKS computational processor would generate an error code because it cannot simultaneously move the beam up and down. As in the case of the planar quadrilateral mechanism, the kinematic study was conducted using `Motion Study` with the `Motion Analysis` submenu.

Figure 12 illustrates the attachment mode of the linear lifting motor to the hydraulic pillar, as well as its characteristics. The motor acts on the piston of the hydraulic pillar along its axis direction. A standard geometric constraint of concentricity has been established between the piston of the hydraulic pillar and the cylinder. The lifting speed along the axis of the piston is constant at 50 mm/s.

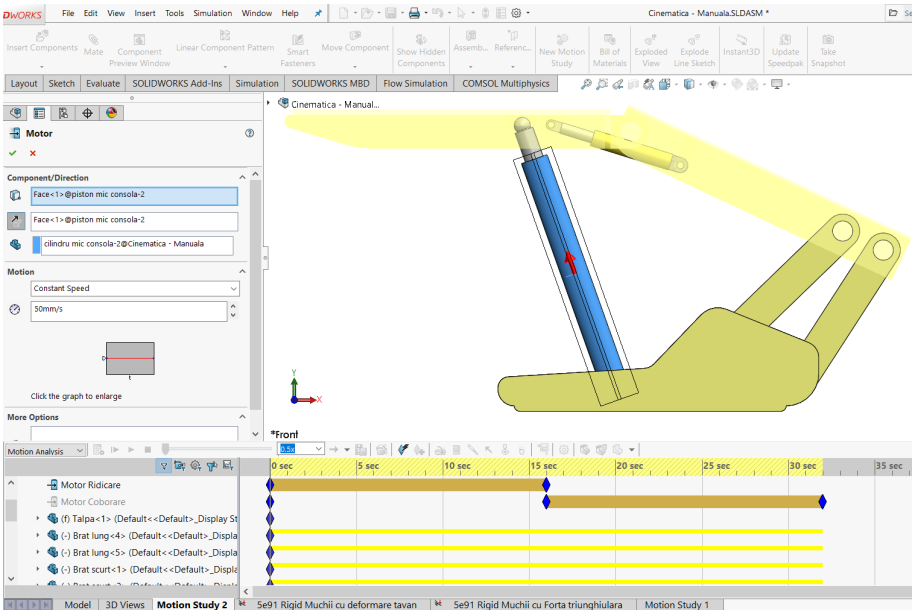

Fig. 12. Attachment of the linear motor to the piston of the hydraulic pillar, along with its characteristics

After performing the calculations, we plotted the trajectory of the shield's tip and the beam's tip of the mechanized support model, as shown in Figures 13.

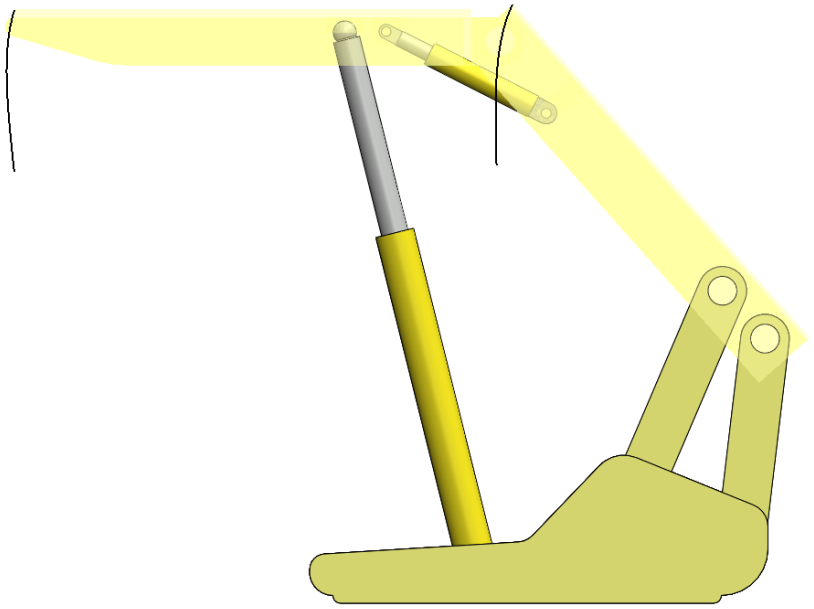

Fig. 13. Trajectories of the shield's tip and the beam's tip of the mechanized support model

After analyzing the shape of the beam tip's trajectory, it can be concluded that it is not a straight line parallel to a vertical plane (face of the mining), but rather a curve with a large radius of curvature that meets the technological requirement for the movement of the beam tip to be nearly vertical. If the condition is imposed that the tip of the support beam maintains the same distance from a vertical plane during lifting, the SOLIDWORKS processor produces a calculation error that stops the simulation.

We utilized the SOLIDWORKS feature to export calculated trajectories into curves belonging to part files. Thus, for the trajectory of the point at the front end of the beam, we created a part where the obtained curve was converted (Convert Entities) into a sketch, resulting in a spline curve. This curve was fitted within a rectangle, as shown in Figure 14.

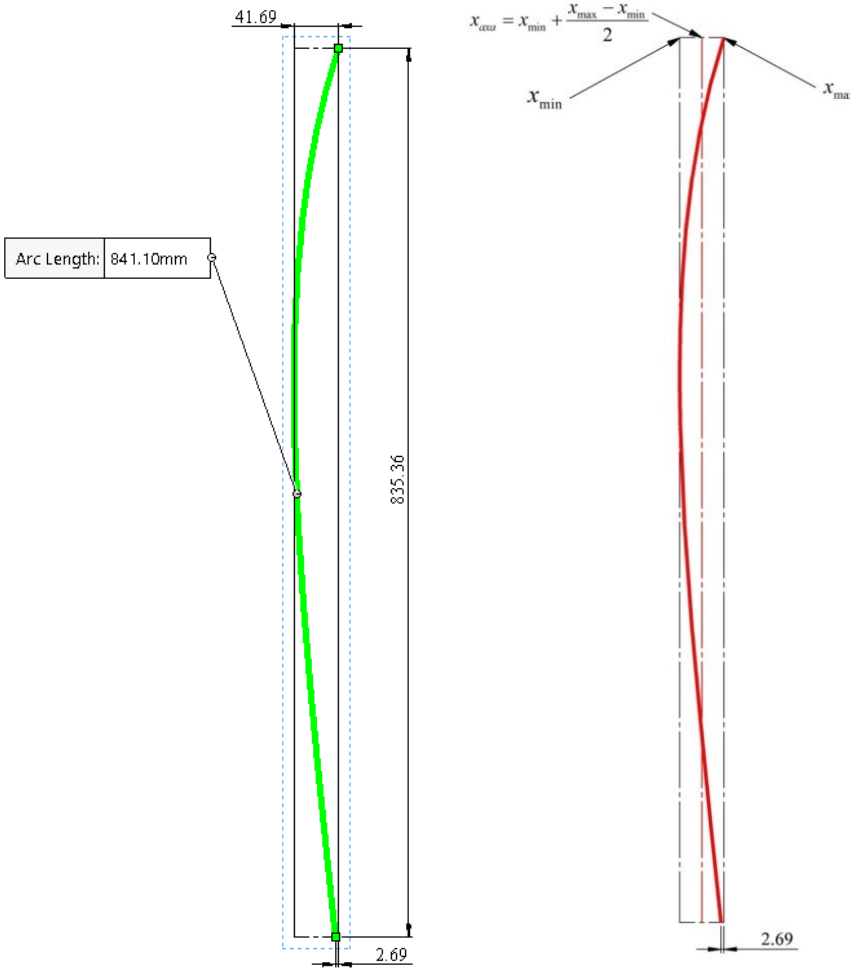

a. b.

Fig. 14. Graphical determination of the dimensions of the trajectory of the point at the front end of the beam, determination of the abscissa of the vertical line

The rectangle was constructed to delineate the limits of the spline curve:
- The left vertical side is tangent to the curve.
- The right vertical side is coincident with the upper right endpoint of the curve.
- The top horizontal side is coincident with the upper right endpoint of the curve.
- The bottom horizontal side is coincident with the lower right endpoint of the curve.

Thus, through a geometric construction, the distance traveled by the point at the front end of the beam in the X and Y directions were determined. These values are 41.69 mm for the X direction and 835.36 mm for the Y direction.

The graphical construction also allowed for the determination of the magnitude of the distance between the abscissa of the initial position of the point and the abscissa of the final position. This distance is 2.69 mm.

To determine the length of the spline curve, the SOLIDWORKS `Evaluate → Measure` feature was used, which, according to Figure 14, is 841.1 mm.

Coordinates of the curve corresponding to the trajectory of the point at the front end of the beam were exported to a `.csv` file. These data were processed in Excel, where the root mean square deviation of the abscissa values of the curve relation to the abscissa value of the vertical line was calculated.

This line is located halfway between the minimum and maximum abscissae of the trajectory (Figure 14. b.). In Excel, the minimum $x_{\min}$ and maximum $x_{\max}$ values of the abscissa series of 402 curves points were determined. The abscissa of the vertical line will be:

$$x_{axa} = x_{\min} + \frac{x_{\max} - x_{\min}}{2} \tag{5}$$

Thus, the root mean square deviation of the abscissae of the curve in relation to the abscissa of the vertical line was calculated:

$$\sigma = \sqrt{\frac{\sum_{i=1}^{n} \left(x_i - x_{axa} \right)^2}{n}} \tag{6}$$

In accordance with the equations (5) and (6), the value of the root mean square is $\sigma = 14,77 \approx 15\,\text{mm}$. Comparing the results obtained through the graphical method presented earlier shows that for the X direction, the deviation is 1.65%, and for the Y direction, it is 0.07%.

4. PLOTTING THE CURVES OF VELOCITY AND ACCELERATION VARIATION FOR THE POINT AT THE FRONT END OF THE BEAM

In Figures 15, 16, and 17, curves depicting the variation over time of the magnitude and components for the X and Y directions of the linear velocity of the point at the front end of the beam of the mechanized support model have been plotted.

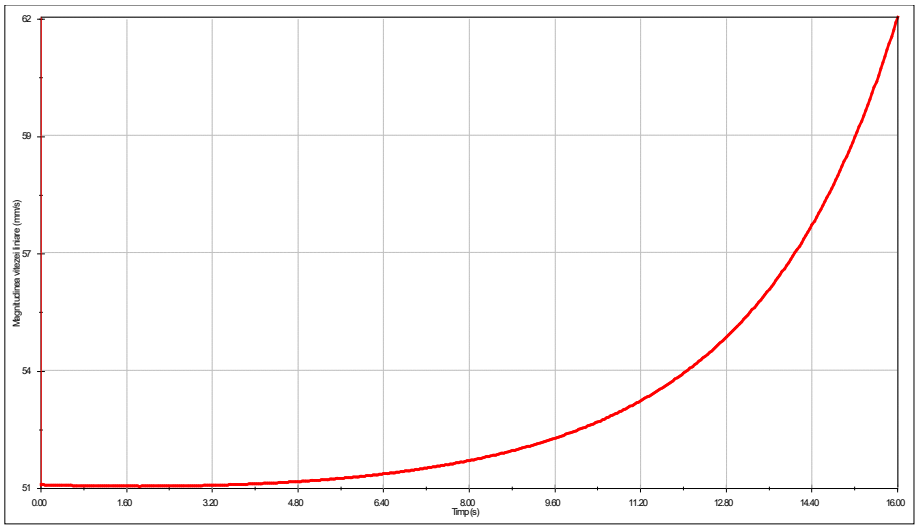

Fig. 15. Variation of the magnitude of linear velocity for the point at the front end of the beam of the mechanized support model

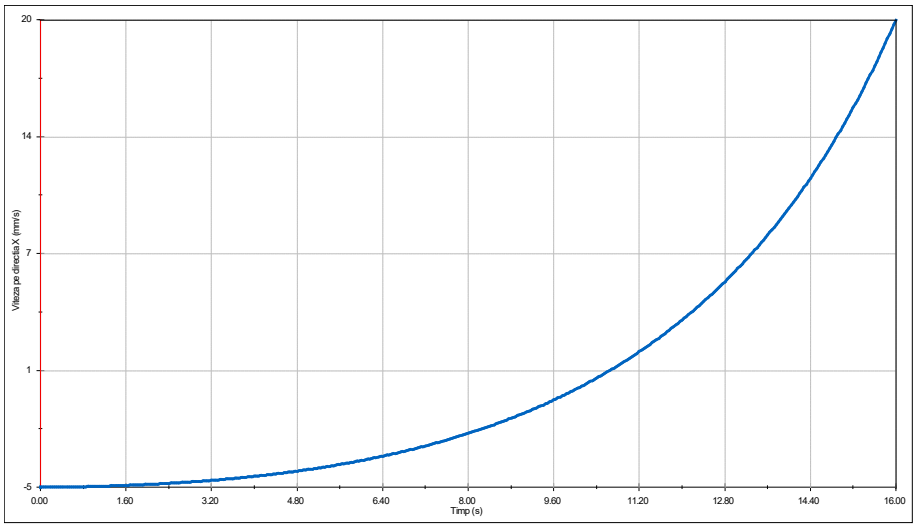

Fig. 16. Variation of the X component of linear velocity for the point at the front end of the beam of the mechanized support model

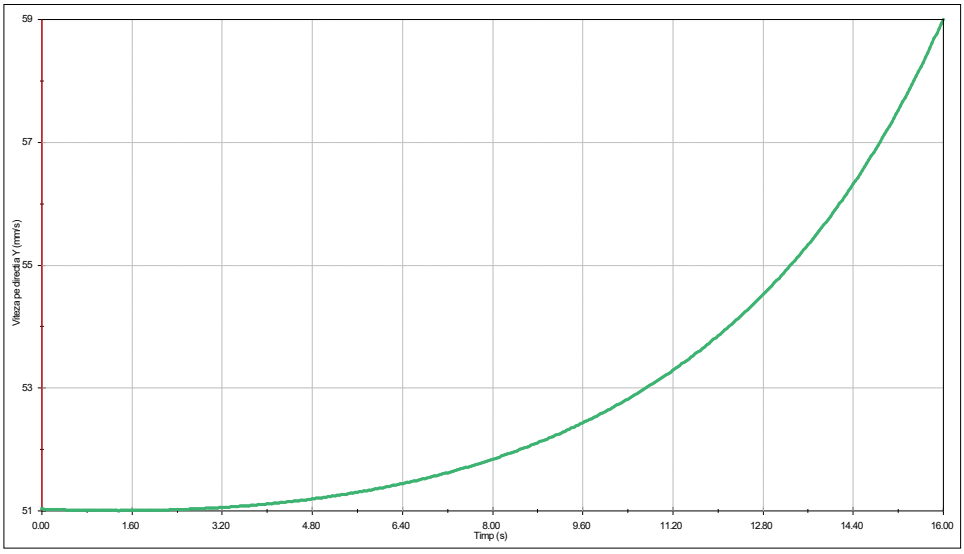

Fig. 17. Variation of the Y component of linear velocity for the point at the front end of the beam of the mechanized support model

For the same point at the front end of the beam of the mechanized support model, diagrams of the variation of accelerations have been plotted. Thus, Figure 18 represents the variation of the magnitude of linear acceleration, while Figures 19 and 20 represent the variation graphs of linear acceleration for the X and Y directions.

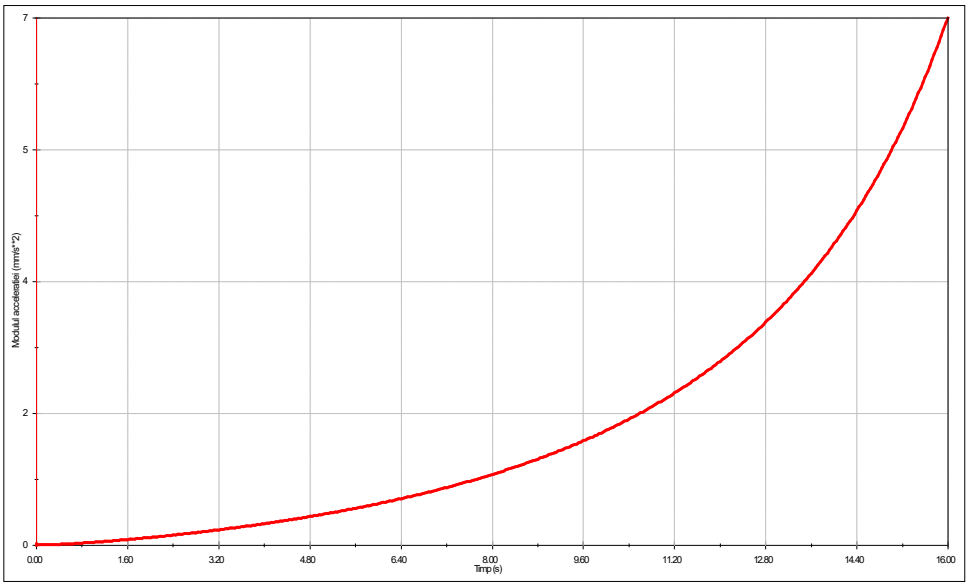

Fig. 18. Variation of the magnitude of linear acceleration for the point at the front end of the beam of the mechanized support model

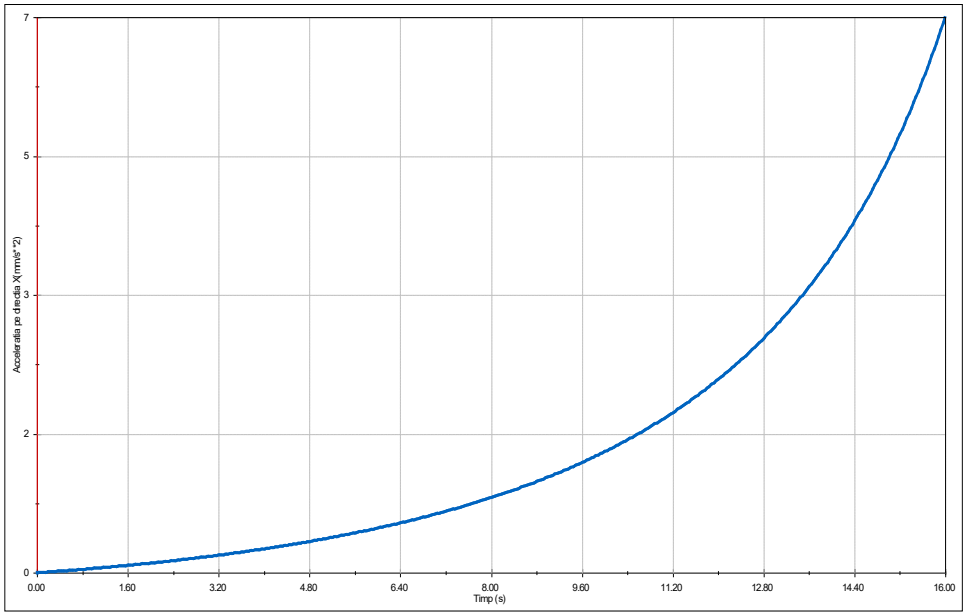

Fig. 19. Variation of the X component of linear acceleration for the point at the front end of the beam of the mechanized support model

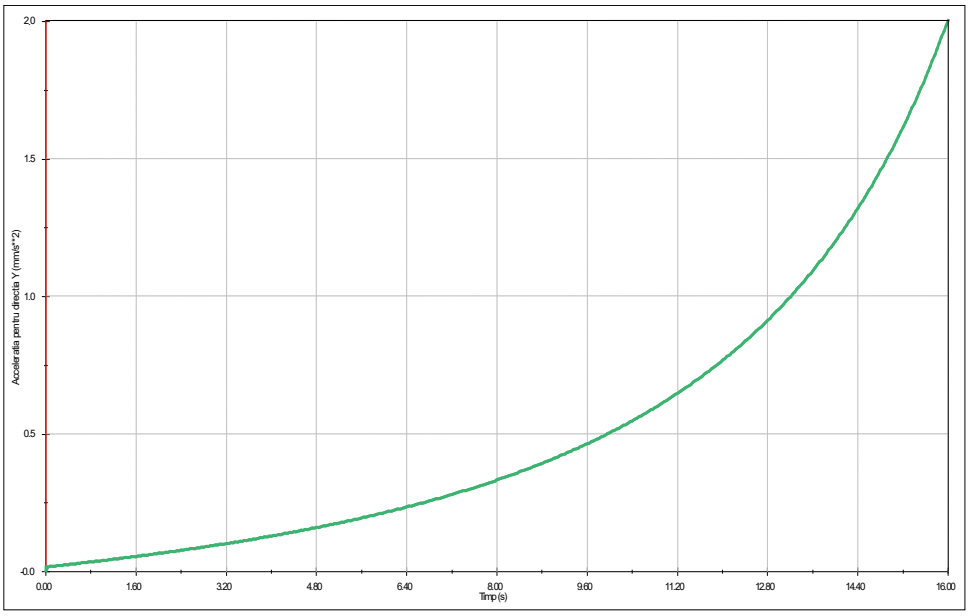

Fig. 20. Variation of the Y component of linear acceleration for the point at the front end of the beam of the mechanized support model

The variation of linear velocities and accelerations of the point at the front end of the beam of the mechanized support is identical to the variation of linear velocities and accelerations (magnitude and components for the X and Y directions) of any point belonging to the piston on which the linear motor acts.

CONCLUSIONS

In this paper, we conducted a theoretical and applied analysis of the geometry and kinematics of the quadrilateral mechanism generating a lemniscate. We demonstrated the utility of using computer-aided modeling and simulation tools to solve these problems. The theoretical part included an analysis of the geometry of generating the lemniscate curve using the parametric equations of the lemniscate in the SOLIDWORKS application.

Subsequently, we performed the kinematic analysis of the quadrilateral mechanism with geometric parameters suitable for its use as a guiding mechanism for the beam. Using the SOLIDWORKS application to generate trajectories, we graphically represented the trajectories described by various points on the driven element, which is structurally assimilated with the support shield.

In the kinematic study of a mechanized support of SMA-2 type using a virtual model, we plotted the trajectory of the shield tip and the beam tip of the mechanized support model. Analyzing the shape of the beam tip trajectory, we concluded that it is not a straight line parallel to a vertical plane (mining face) but a curve with a large radius of curvature that meets the technological requirement for the movement of the beam tip to be nearly vertical.

Using trajectory data and the Excel utility, we calculated the root mean square deviation of the abscissa values of the curve relative to the abscissa value of the vertical line. Analyzing the deviation values determined in this way compared to those obtained through analytical methods, we demonstrated the utility and relevance of the proposed kinematic analysis method.

In summary, the main conclusions drawn are as follows:

- In planar quadrilateral mechanisms, the point at the free end of the connecting rod-like driven element describes a lemniscate trajectory when the driving element acts as a crank;
- Conditions for a planar quadrilateral mechanism to function as a crank are:
  - The shortest element in the mechanism should either be the driving element or the fixed base;
  - The sum of the minimum and maximum lengths of the elements should be equal to the sum of the lengths of the other two elements;
- In the case of a quadrilateral mechanism with a crank, the main points on the connecting rod-like element describe:
  - A symmetrical lemniscate for the point at the free end of the rod;
  - Asymmetrical lemniscates for points between the maximum end point and the pivot point with the crank;

  - A circle for the pivot point with the crank;
  - Closed curves for points between the pivot point with the crank and the pivot point with the rocker;
  - An arc of a circle for the pivot point with the rocker.
- For the SMA-2 mechanized support model, the quadrilateral mechanism consists of a base, the supporting arms of the shield, and the shield itself;
- The dimensional parameters of the quadrilateral mechanism corresponding to the mechanized support adhere to Grashof's condition and represent a double rocker mechanism;
- The lifting of the mechanized support beam through a linear actuator acting on the hydraulic post piston along its axis results in a lemniscate trajectory of the front tip of the beam;
- During the process of lifting the mechanized support, the dimensional characteristics of the technological space for the X and Y directions were determined using numerical and graphical methods. The difference between the obtained results is 1.65% for the X direction, and for the Y direction, it is 0.07%;
- Since the root mean square deviation of the abscissa values of the trajectory of the point at the front end of the beam, relative to the abscissa of a vertical line situated midway between the minimum and maximum abscissa values of the trajectory, is small (approximately 15 mm), considering the large displacement in the Y direction, it can be considered technically that the trajectory is nearly a vertical line;
- The variation diagrams of the linear velocity magnitude and components for the X and Y directions exhibit a parabolic variation over the simulation time interval;
- The variation diagrams of the linear acceleration magnitude and components for the X and Y directions exhibit a parabolic variation over time.

REFERENCES

[1]. **Kurowski, P.,M.**, *Engineering Analysis with SOLIDWORKS® Simulation 2015*.
[2]. **Kurowski, P.,M.**, *Vibration Analysis with SOLIDWORKS® Simulation 2016*.
[3]. **Popescu, F.D.** *Controls ways of the transportation capacity variation for the canvas conveyer*. WSEAS Transactions on Systems and Control, 2008, (5), p.393.
[4]. **Mihailescu S.**, *Utilaje de transport pe calea ferata pentru* subteran, ISBN: 978-973-741-035-1, Editura Universitas, Petroşani, 2006.
[5]. **Popescu, F. D., Radu, S.M., Andras, A., Kertesz, I.** *Infografică, modelare şi simulare asistată de calculator – format electronic*, Editura Universitas, Petroşani, 2020, ISBN 978-973-741-715-2.
[6]. **Radu, S.M., Popescu, F.D., Andras, A., Kertesz, I.**, *Transport si instalaţii miniere*, Editura Universitas, Petroşani, 2018, ISBN 978-973-741-587-5.

[7]. **Sham Tickoo**, *SOLIDWORKS Simulation 2016: A Tutorial Approch, CDCIM Techologies*, Schereville, Indiana 46375, USA.
[8]. **Popescu, F.D.** *Instalaţii de Transport pe Vertical*, Editura Focus: Petroșani, Romania, ISBN 978-973-677-182-8, 2010.
[9]. **Virág, Z.** *Determination of optimum diameter of a welded stiffened cylindrical shell*. Pollack Periodica, 2009, 4(1), pp.41-52.
[10]. **Andras, I., Radu, S. M., Andras, A.,** *Study Regarding the Bucket-Wheel Excavators Used in Hard Rock Excavations,* Annals of the University of Petroşani, Mechanical Engineering, Vol. 18, pp. 11-22, (2016)
[11]. **Popescu, F.D.** *Calculatorul numeric în industria extractivă*, Editura Universitas, Petroşani, 2004.
[12]. **Popescu, F.D.** *Aplicaţii industriale ale tehnicii de calcul*, Editura AGIR, Bucureşti, 2009.
[13]. **Virág, Z., Szirbik, S.** *Finite element modal analysis of a hybrid stiffened plate*. Ann. Univ. Petroşani Mech. Eng. 2019, 21, 115–120.
[14]. **Radu, S. M., Chmielarz, W., Andras, A.** *Mining Technological System's Performance Analysis.* Annals of the University of Craiova for Journalism, Communication and Management, 2(1), pp. 56-64, (2016).